JACS
JOURNAL OF THE AMERICAN CHEMICAL SOCIETY
Communication
pubs.acs.org/JACS

Enhanced Photocatalytic CO_2-Reduction Activity of Anatase TiO_2 by Coexposed {001} and {101} Facets

Jiaguo Yu,*[,†] Jingxiang Low,[†] Wei Xiao,[†] Peng Zhou,[†] and Mietek Jaroniec*[,‡]

[†]State Key Laboratory of Advanced Technology for Material Synthesis and Processing, Wuhan University of Technology, Luoshi Road 122#, Wuhan 430070, P. R. China

[‡]Department of Chemistry and Biochemistry, Kent State University, Kent, Ohio 44242, United States

Supporting Information

ABSTRACT: Control of TiO_2 crystal facets has attracted enormous interest due to the fascinating shape-dependent photocatalytic activity of this material. In this work, the effect of the ratio of {001} and {101} facets on the photocatalytic CO_2-reduction performance of anatase TiO_2 is reported. A new "surface heterojunction" concept is proposed on the basis of the density functional theory (DFT) calculations to explain the difference in the photocatalytic activity of TiO_2 with coexposed {001} and {101} facets.

In response to the increasing environmental and energy-related concerns, production of chemical fuels utilizing renewable solar energy is considered as a promising approach.[1,2] Particularly, the use of solar energy to trigger photocatalytic reduction of CO_2 into valuable organic fuels, such as methane, formic acid, and methanol, is of particular interests because of its capability of mimicking natural photosynthesis to convert solar energy into chemical energy.[3,4] Nowadays, there is an enormous interest in controlling titania crystal facets due to their fascinating shape-dependent physicochemical properties.[5−7] Generally, most anatase TiO_2 crystals feature the exposed {101} facets rather than {001} facets due to higher thermodynamic stability of the former.[8] According to the Wulff construction (see Figure S1 in Supporting Information), the less reactive and more thermodynamically stable {101} facets constitute about 90% of the total exposed surface of the naturally occurring anatase TiO_2.[9,10] Therefore, unusual physicochemical properties can be expected for anatase with high-surface-energy exposed {001} facets. For example, Lu et al. reported an important breakthrough in the synthesis of anatase TiO_2 single crystals with high percentage of exposed {001} facets by using F^- as a stabilizing agent.[11] Afterward, Han et al. found that {001} facets exhibit higher photocatalytic activity than {101} facets due to the high density of active unsaturated Ti atoms and active surface oxygen atoms on {001} facets.[9] These anatase TiO_2 crystals with high ratio of the exposed {001} facets have a great potential in applications ranging from solar cells, photonic and optoelectronic devices, and sensors to photocatalysis.[7]

Herein, we report for the first time the photocatalytic reduction of CO_2 over anatase TiO_2 with coexposed {001} and {101} facets and the effect of the ratio of these facets on the aforementioned reduction process. Further, a new "surface heterojunction" concept is proposed on the basis of the DFT calculations to explain the difference in the photocatalytic activity of anatase TiO_2 with coexposed {001} and {101} facets.

The schematic geometrical structures of the optimized 2 × 2 × 1 supercells of the exposed {001} and {101} surface of anatase TiO_2 are illustrated in Figure S2 (Supporting Information). In particular, {001} surface shows larger Ti−O−Ti bond angles, while {101} surface features lower Ti−O−Ti bond angles.[12] With larger Ti−O−Ti bond angle, 2p states of the surface O atoms on {001} facets are destabilized and very reactive.[10] The DFT electronic structure calculations of {001} and {101} facets are shown in Figure 1a. As can be seen from this figure, the Fermi level of {001} facets enter their valence band. However, the Fermi level of {101} facets is still located at the top of the valence band of {101} surface. Because {001} and {101} facets contact each other, their Fermi levels should be equal. So, it is not surprising that the {001} and {101} surfaces can form surface heterojunction (see Figure 1b), which is beneficial to the transfer and separation of photogenerated electrons and holes. Therefore, the photogenerated electrons and holes migrate to {101} and {001} facets during the photocatalytic process, respectively.[7,13] Consequently, the ratio of the exposed {101} and {001} facets has a pronounced effect on the photocatalytic activity of anatase TiO_2.

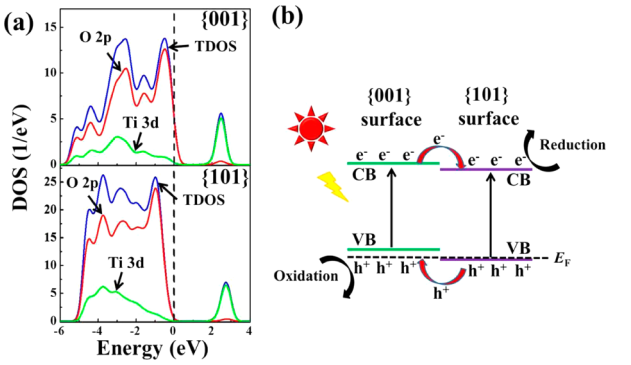

Figure 1. (a) Density of states (DOS) plots for {101} and {001} surface of anatase TiO_2. O 2P, Ti 3d, and TDOS are partial DOS of O 2P, partial DOS of Ti 3d, and total DOS, respectively. (b) {001} and {101} surface heterojunction.

Received: January 29, 2014
Published: June 11, 2014

   dx.doi.org/10.1021/ja5044787 | J. Am. Chem. Soc. 2014, 136, 8839−8842

A series of anatase TiO_2 with different ratios of the exposed {101} and {001} facets were prepared, and the percentage of {001} facets was calculated as reported elsewhere[14] (see experimental, Figure S3 and Table 1 in Supporting Information). Figure S4 (Supporting Information) shows the XRD patterns of the anatase TiO_2 formed using different amounts of HF. The prepared TiO_2 was a well-crystallized anatase and the main diffraction peaks in the pattern are identical with the standard card [JCPDS No. 21-1272, space group: *I*41/*amd* (141)].[15] It is noteworthy that with increasing amount of HF, the XRD peak intensities of the samples steadily increase and the widths of the XRD peaks become narrower, indicating the enhancement of TiO_2 crystallization. This is consistent with our previous report that fluoride improves the crystallization of anatase phase and enhances the growth of crystallites.[15] According to the experimental results and theoretical estimation of the XRD patterns, the physicochemical properties of the prepared samples are summarized in Table 1.

Table 1. Physicochemical Properties of Different Samples

sample	HF (mL)	phase	{001} facets %	RC[a]	CH_4 production (μmol h^{-1} g^{-1})
HF0	0	A	11	1	0.15
HF3	3	A	49	1.26	0.75
HF4.5	4.5	A	58	1.35	1.35
HF6	6	A	72	1.51	0.82
HF9	9	A	83	1.67	0.55
P25	-	A, R	-	-	0.38

[a]RC: Relative crystallinitiy, the relative intensity of diffraction peak from the anatase {101} facets (reference = HF0).

Naturally, anatase TiO_2 is a truncated octahedral bipyramid comprising of eight {101} facets on sides and two {001} facets on the top and bottom (see Figure S1 in Supporting Information). As shown in the transmission electron microscopy (TEM) images (Figure 2a), the shape of HF0 is similar to that of the natural anatase, which is octahedral bipyramid with an average side length of ca. 13 nm and width of ca. 11 nm. By adding 4.5 and 9 mL of HF into the precursor (see Figure 2b,c), the sample turns into nanoplates. HF4.5 has an average side length of ca. 80 nm and thickness of ca. 30 nm, while HF9 has an average side length of ca. 100 nm and thickness of ca. 6 nm, indicating the enhancement of crystallization and the formation of greater crystallites. This is in a good agreement with the above XRD results. Moreover, it is obvious that HF4.5 and HF9 feature the larger percentage of the exposed {001} facets in comparison to that of HF0, indicating that F^- plays a key role in the formation of TiO_2 nanoplates with high percentage of the exposed {001} facets (see Table 1).

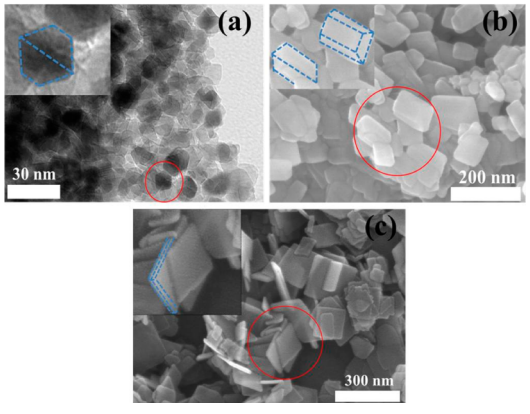

Figure 2. (a) TEM image of HF0 and (b and c) FESEM images of HF4.5 and HF9. The insets show the enlarged images of (a) HF0, (b) HF4.5, and (c) HF9.

Figure S5 in Supporting Information presents the XPS survey spectra of HF0 and HF4.5. The Ti, O, and C elements are clearly observed in the XPS spectra of both HF0 and HF4.5. However, no F element is observed, indicating that the surface fluoride introduced by HF was completely removed by annealing method. Figure S6 in Supporting Information shows the UV–visible absorption spectra of the HF0, HF4.5 and HF9 samples. The onsets of the absorption edge for HF0 is at ca. 390 nm, which is consistent with the bandgap of anatase TiO_2 (~3.2 eV). Moreover, no obvious changes at the absorption edge are observed for the HF4.5 and HF9 samples, indicating that the bandgaps of three samples are similar.

The Brunauer–Emmett–Teller (BET) specific surface area (S_{BET}) and pore structure of the prepared samples were investigated using nitrogen adsorption–desorption measurements (see Table S1 in Supporting Information). Figure S7 in Supporting Information presents the nitrogen adsorption–desorption isotherms and the corresponding pore size distribution curves for HF0 and HF4.5. Type IV isotherms are observed, indicating the presence of mesopores (2–50 nm) formed between anatase nanocrystals. Figure S8 in Supporting Information shows a comparison of the electrochemical impedance spectra (EIS) of the samples. As can be seen from this figure, the diameter of the semicircle decreases from HF0 to HF4.5, indicating that the appropriate ratio of the exposed {001} and {101} facets could significantly reduce the recombination rate of photoinduced electrons and holes. However, HF6 and HF9 exhibit a significant increase in the semicircle diameter as compared to that of HF4.5. This is due to further increase in the amount of HF, which led to the higher percentage of the exposed {001} facets on the sample, which play the role of recombination centers for photogenerated charge carriers and thus inhibit the charge separation.

Finally, the photocatalytic CH_4-production performance of the prepared TiO_2 was investigated, and the results are shown in Figure 3. As can be seen from this figure, the photocatalytic activity of the TiO_2 samples studied is strongly affected by the

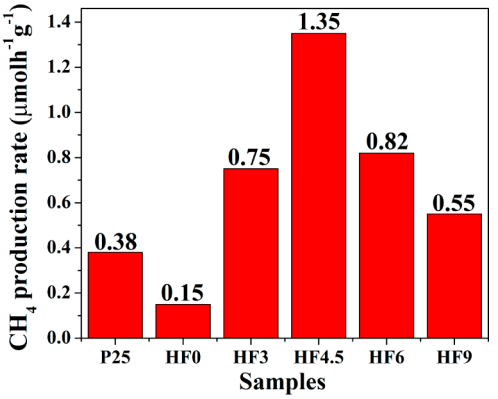

Figure 3. Comparison of the photocatalytic CH_4-production activity of P25 and the TiO_2 samples prepared by varying HF amount.

dx.doi.org/10.1021/ja5044787 | J. Am. Chem. Soc. 2014, 136, 8839–8842

ratio of the exposed {001} to {101} facets. For HF0, a relatively low photocatalytic CH_4-production rate (0.15 μmol h^{-1} g^{-1}) was observed because the rapid recombination of CB electrons and VB holes. By increasing the HF amount from 3 to 4.5 mL, the photocatalytic activity of the samples gradually increased, indicating that this increase is affected by the presence of larger amount of {001} facets. In particular, the highest CH_4-production rate, obtained for HF4.5, is 1.35 μmol h^{-1} g^{-1}. This value exceeds that of HF0 by a factor of 9. However, a further increase of HF amount (6 and 9 mL) caused a reduction in the photocatalytic activity. This is due to a large amount of the exposed {001} facets in anatase, which causes an electron overflow effect on {101} facets due to their lower percentage. As a result, the electrons on the {001} facets and within the interior are hardly transferred to {101} facets and easily recombine with holes on the {001} facets due to their dominance. The relation between the exposed {001} facets and the CH_4 production rates is summarized in Table 1. As can be seen in this table, HF4.5 shows a 3- and 9-fold photocatalytic activity improvement over commercial TiO_2 P25 and HF0, respectively. The superior activity of HF4.5 was achieved by optimizing the ratio of the {001} and {101} facets.

A comparison of the amounts of produced CH_4 expressed per unit surface area permits to see the difference in the catalytic activity among the samples studied; namely, these amounts measured for the HF0, HF4.5, and HF9 samples are 1.4×10^{-3}, 30×10^{-3}, and 18.3×10^{-3} μmol h^{-1} m^{-2}, respectively (see Table S1 in Supporting Information). Certainly, the observed large difference in the catalytic activity per unit surface area is caused by surface heterojunctions, not by the specific surface area and crystallinity. For example, the corresponding surface areas and crystallinities for the HF0 and HF4.5 samples are 107 and 45 m^2/g, and 1 and 1.35, respectively. Usually, a decrease in the specific surface area reduces the specific photocatalytic activity (expressed per unit mass of the catalyst). Contrarily, an increase in the crystallinity enhances this activity. Obviously, these two factors cannot cause such great 21-fold increase in the catalytic activity, from 1.4×10^{-3} to 30×10^{-3} μmol h^{-1} m^{-2}. The only explanation remains the effect of surface heterojunctions.

On the basis of the above experimental results and theoretical analysis, a simple mechanism explaining the observed enhancement in the photocatalytic activity of HF4.5 is proposed (see Figure 4). When the samples are irradiated by light, the VB electrons of anatase are excited to the CB level, while holes remain in VB. For HF0, the most of electrons and holes are mainly accumulated on the {101} facets due to the low percentages of {001} facets. Consequently, the charge carriers easily recombine and only a small fraction of electrons and holes participate in the photocatalytic reaction. With increasing amount of HF to 4.5 mL (HF4.5 sample), an optimal percentage of the exposed {001} and {101} facets is achieved. In this case, the electron and hole pairs can efficiently migrate to {101} and {001} facets, respectively. Thus, {101} facets act as reduction sites, while {001} facets act as oxidation sites on the anatase surface. As a result, the optimal ratio of {001} and {101} facets significantly enhances the photocatalytic activity. However, a further increase in the amount of the {001} facets on the TiO_2 surface may cause an electron overflow effect toward {101} facets. Thus, the migration of electrons to {101} facets is more difficult due to their low population. Therefore, it is not surprising that the photocatalytic activity of HF9 is significantly reduced as compared to that of HF4.5.

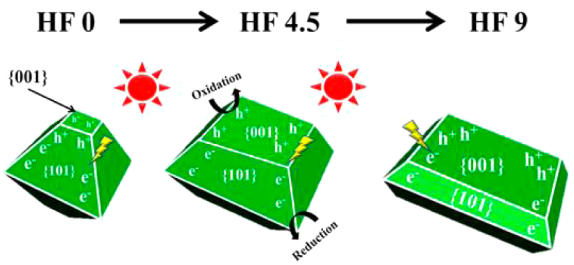

Figure 4. Schematic illustration of the spatial separation of redox sites on the HF0, HF4.5, and HF9 samples.

In summary, based on the DFT calculations, we showed that the {101} and {001} facets of anatase TiO_2 exhibit different band structures and band edge positions. Thus, the coexposed {101} and {001} facets of anatase can form a surface heterojunction within single TiO_2 particle, which is beneficial for the transfer of photogenerated electrons and holes to {101} and {001} facets, respectively. Therefore, it is easy to understand that the ratio of the exposed {101} and {001} facets greatly affects the photocatalytic activity of anatase toward reduction of CO_2 to CH_4. The optimal ratio of the exposed {101} and {001} facets was determined to be 45:55. This finding not only explains the importance of the optimal ratio of the exposed {101} and {001} facets on the enhancement of photocatalytic performance of TiO_2, but also provides a new insight into the design and fabrication of advanced photocatalytic materials.

■ ASSOCIATED CONTENT

Supporting Information

Experimental procedures and additional data. This material is available free of charge via the Internet at http://pubs.acs.org.

■ AUTHOR INFORMATION

Corresponding Authors

jiaguoyu@yahoo.com
jaroniec@kent.edu

Notes

The authors declare no competing financial interest.

■ ACKNOWLEDGMENTS

This work was supported by the 973 program (2013CB632402) and NSFC (51272199, 51320105001, 51372190 and 21177100).

■ REFERENCES

(1) Fujishima, A.; Honda, K. *Nature* **1972**, *238*, 37.
(2) Xiang, Q.; Yu, J.; Jaroniec, M. *J. Am. Chem. Soc.* **2012**, *134*, 6575.
(3) Xie, S.; Wang, Y.; Zhang, Q.; Fan, W.; Deng, W. *Chem. Commun.* **2013**, *49*, 2451.
(4) Wang, W.; Wang, S.; Ma, X.; Gong, J. *Chem. Soc. Rev.* **2011**, *40*, 3703.
(5) Wen, C. Z.; Zhou, J. Z.; Jiang, H. B.; Hu, Q. H.; Qiao, S. Z.; Yang, H. G. *Chem. Commun.* **2011**, *47*, 4400.
(6) Dai, Y.; Cobley, C. M.; Zeng, J.; Sun, Y.; Xia, Y. *Nano Lett.* **2009**, *9*, 2455.
(7) Liu, S.; Yu, J.; Jaroniec, M. *Chem. Mater.* **2011**, *23*, 4085.
(8) Liu, S. W.; Yu, J. G.; Jaroniec, M. *J. Am. Chem. Soc.* **2010**, *132*, 11914.
(9) Han, X.; Kuang, Q.; Jin, M.; Xie, Z.; Zheng, L. *J. Am. Chem. Soc.* **2009**, *131*, 3152.

(10) Selloni, A. *Nat. Mater.* **2008**, *7*, 613.
(11) Yang, H. G.; Sun, C. H.; Qiao, S. Z.; Zou, J.; Liu, G.; Smith, S. C.; Cheng, H. M.; Lu, G. Q. *Nature* **2008**, *453*, 638.
(12) Pan, J.; Liu, G.; Lu, G. Q.; Cheng, H. M. *Angew. Chem., Int. Ed.* **2011**, *50*, 2133.
(13) Zheng, Z.; Huang, B.; Lu, J.; Qin, X.; Zhang, X.; Dai, Y. *Chem.—Eur. J.* **2011**, *17*, 15032.
(14) Xiang, Q. J.; Yu, J. G.; Jaroniec, M. *Chem. Commun.* **2011**, *47*, 4532.
(15) Xiang, Q. J.; Lv, K. L.; Yu, J. G. *Appl. Catal., B* **2010**, *96*, 557.